# Calibration campaign of the Borexino detector for the search of sterile neutrinos with SOX


L. Collica[1], D. Bravo Berguño[1,2], K. Choi[3], M. Nieslony[4]
(on behalf of the Borexino Collaboration)

[1] INFN Milano, [2] Virginia Tech, [3] University of Hawaii, [4] University of Mainz


## Introduction

The SOX (Short distance Oscillation with boreXino) experiment aims to investigate possible anomalous oscillatory behaviour in neutrinos, including the existence of sterile neutrinos, by looking for a rate deficit in the observed antineutrino rate and an explicit oscillation pattern in space and energy. Observing this pattern would be a "smoking gun" evidence for the existence of sterile neutrinos. A new calibration campaign is crucial to achieve a deeper understanding of the energy response and the spatial reconstruction accuracies of the detector. Differently from the 2008-2010 campaign, which was focused on solar neutrino analysis, there will be an extensive calibration in the whole active volume and with different source types specifically chosen for SOX's analysis.

## The Borexino/SOX project

The Borexino experiment [1] is located deep underground at the Gran Sasso Laboratory (3800 m.w.e.) in Italy. It consists of a large volume, liquid scintillator (PC+PPO) detector and its primary purpose is the real-time measurement of low-energy solar neutrinos [2]. Its unique properties make it also suitable for the investigation of a possible sterile neutrino state in the SOX experiment [3].

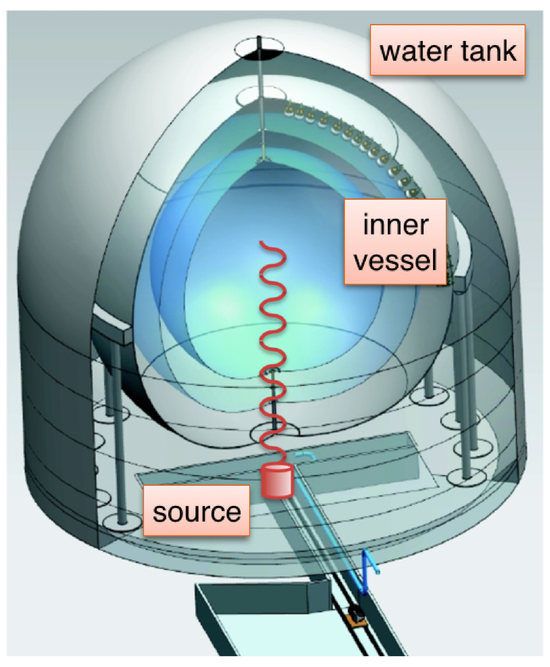


Features of SOX:

- $^{144}$Ce-$^{144}$Pr anti-neutrino source placed 8.5 m below the Borexino detector
- sensitive to $\Delta m^2_{14} \approx 1eV^2$
- start data taking: January - April 2018
- time frame: 1.5 years
- expected number of total events: $\approx$ 10,000
- source activity: 100-150 kCi
- energy reconstruction: $\sigma = 5\%$ at 1 MeV
- position reconstruction: $\sigma$ = 10 cm at 1 MeV

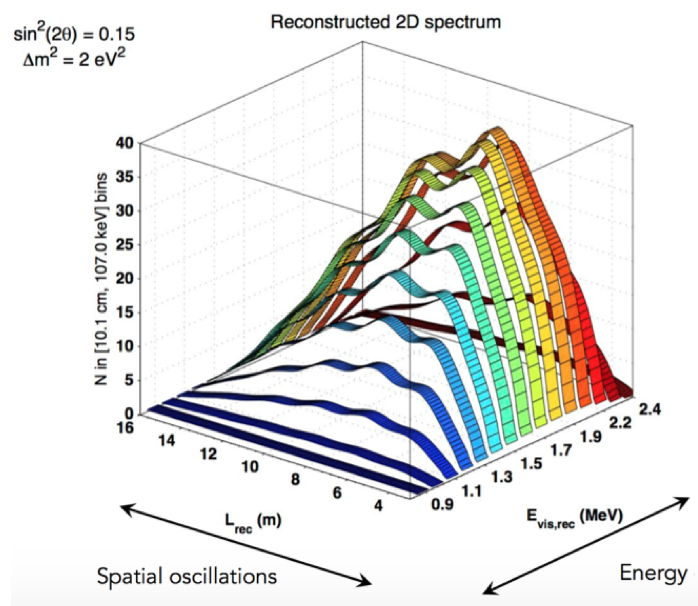


## Motivations

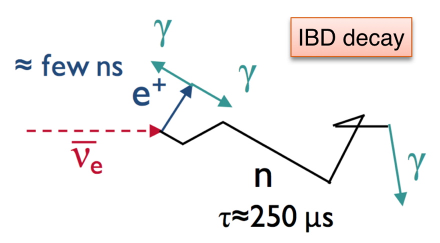


Anti-neutrinos are detected inside Borexino via inverse beta decay, providing a clear coincidence signature with a prompt positron annihilation and a delayed neutron capture.

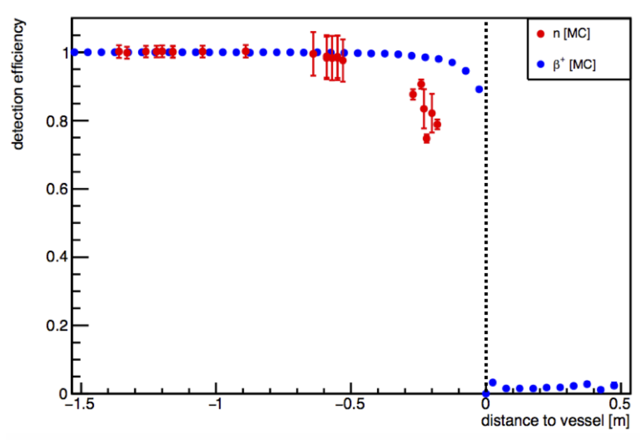

**Events at the border** do not deposit their whole energy in the scintillator, but experience energy losses in the non-scintillating buffer. The resulting efficiencies are depicted for the neutron calibration source (red) and the positron calibration source (blue), based on Monte Carlo simulations.

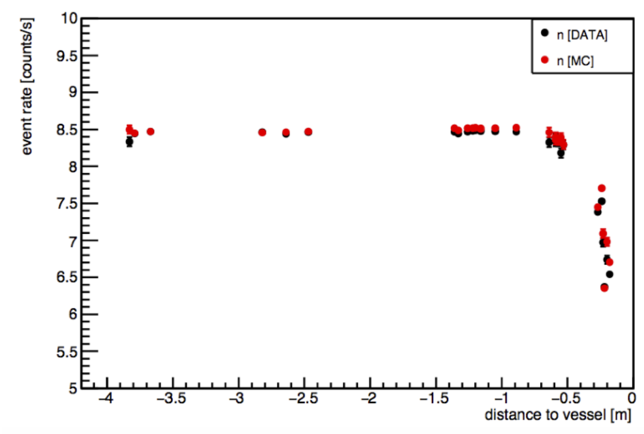

**Monte Carlo - data agreement** for the neutron calibration source is <2% for the central part of the detector while it reaches up to 4% for events which are closer than 50 cm to the vessel border.

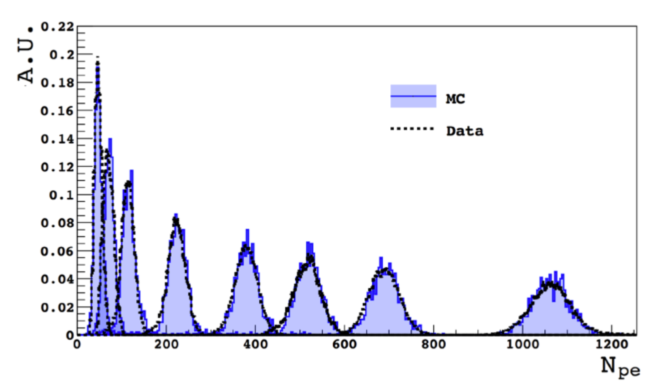

**The last calibration campaign** in 2009 provided excellent agreement between Monte Carlo and data for the energy spectra of the $\gamma$ calibration sources. However, only the low energy sources, important for the solar neutrino analysis, were used.

## Calibration layout - 3D model

To plan and visualise the different scans (on-axis, off-axis, $\phi$ and radial), a flexible 3D model has been developed. Features:

- equidistant scheme with distances from 4.5 m to 9.25 m from the pit;
- radial scans for efficiency mapping;
- $\phi$-scans to check for a possible vessel asymmetry;
- total of 245 calibration points for the neutron source; a subset of them will be used for the other sources;
- more calibration points in the South compared to the North (flux considerations).

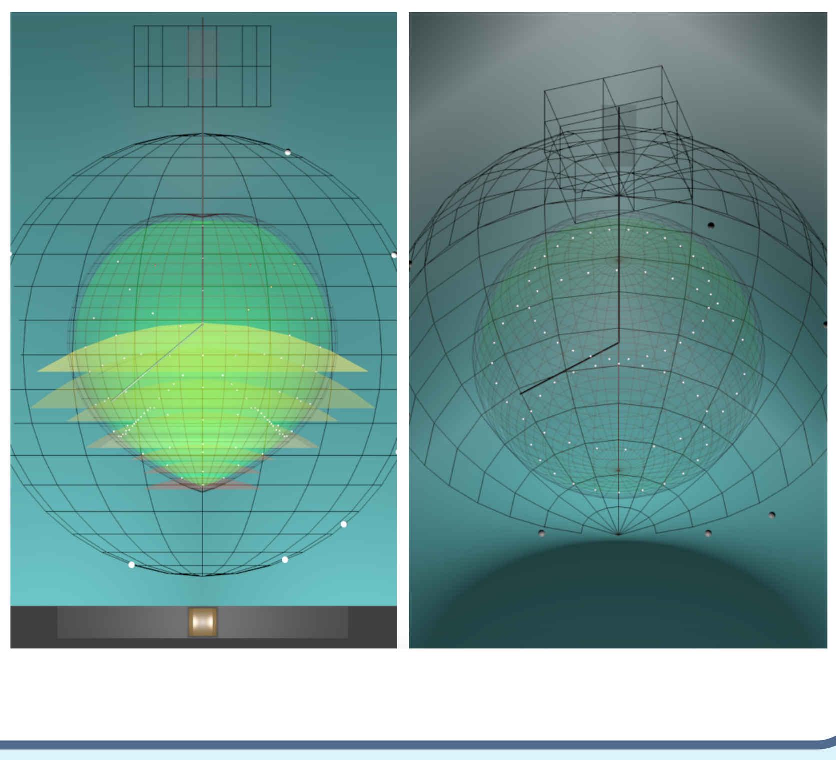

## Setup and system handling

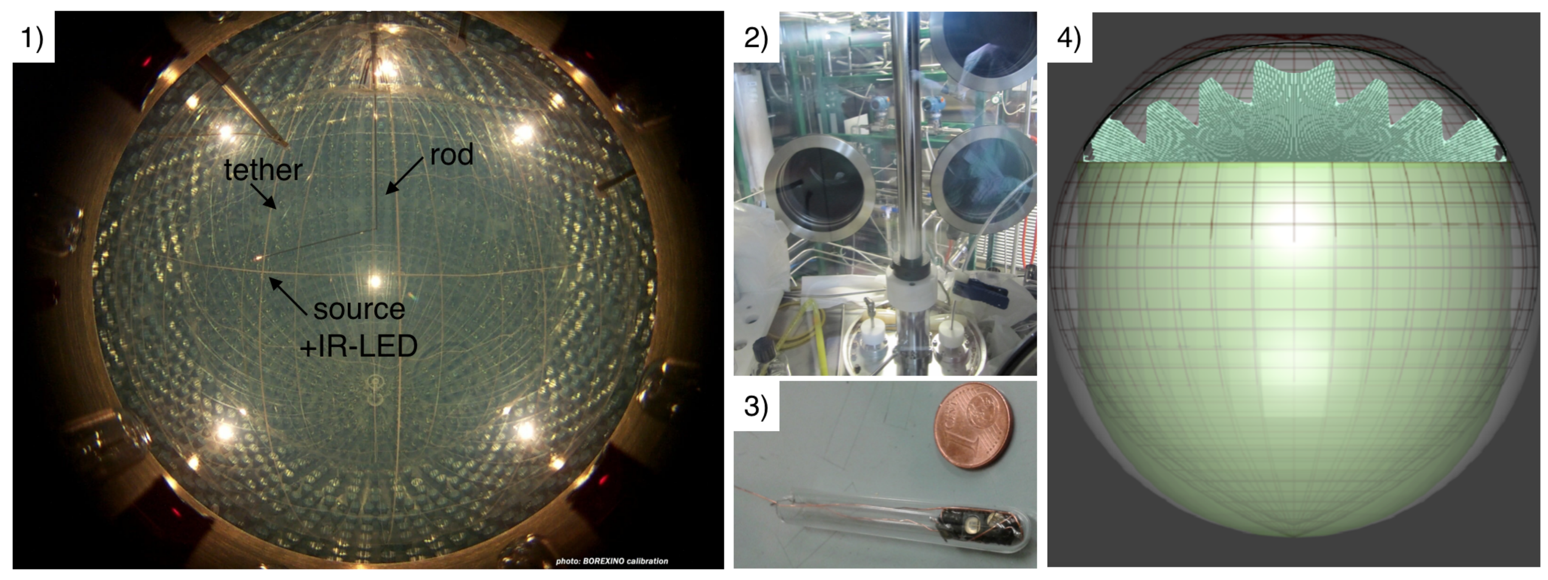


- insertion of sources via series of interconnecting rods (3.8 cm x 100 cm);
- a Teflon tether tube enters the detector alongside the rods and it is used to adjust the hinge angle to the desired position (see Figure 1);
- arm segments can be added or removed and $\phi$-rotations can be performed;
- entire system housed in clean room to avoid perturbing radio-purity of the detector;
- all manipulation performed inside of Low Argon and Krypton Nitrogen (LAKN) filled glove box to minimise radon contamination (see Figure 2);
- source location system composed of 6 CCD cameras looking for the position of a IR-LED attached to the source (see Figure 3), characterised by a precision of about 1 cm in the center of the vessel;
- the source can be deployed in almost the whole scintillator volume: to avoid touching the vessel a safety distance of 15-20 cm from it will be kept while due to hardware constraints (tether, mechanics) some region will not be reachable (see Figure 4).

## Calibration sources

| Source | Type | E [MeV] | scan |
|---|---|---|---|
| $^{241}$Am$^{9}$Be(+$^{nat}$Ni) | n | 0-9 | on-axis, off-axis radial, $\phi$ |
| $^{222}$Rn | $\alpha$ | 5.5, 6.0, 7.4 | on-axis, off-axis, $\phi$ |
| | $\gamma$ | 0-3.2 | on-axis, off-axis, $\phi$ |
| $^{68}$Ge $-^{68}$ Ga | $\beta^+$ | 0-1.9 (+1.02) | on-axis, off-axis radial, $\phi$ |
| $^{85}$Sr, $^{54}$Mn, $^{65}$Zn, $^{40}$K | $\gamma$ | 0.5, 0.8, 1.1, 1.5 | on-axis |
| $^{60}$Co-$^{108m}$Ag | $\gamma$ | 1.2-1.3, 0.4-0.6-0.7 | on-axis |

- extensive calibration with neutron source to map neutron detection efficiency and energy response;
- $\alpha$ and $\beta^+$ sources will be used to respectively map accuracy of the position reconstruction and the positron detection efficiency;
- mono-energetic $\gamma$ sources to map energy response on-axis;
- an UV LED system will also be used for the energy calibration of FADC at high energies.

## Calibration vials

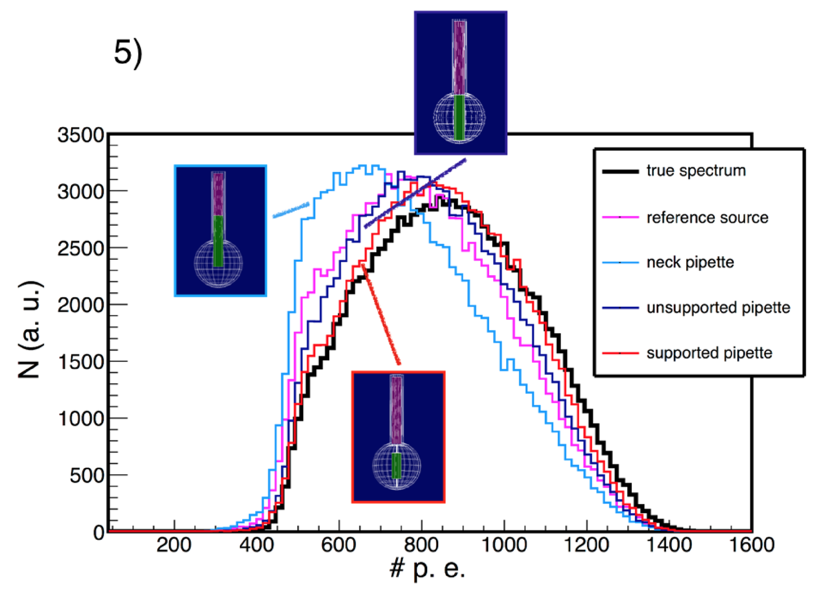



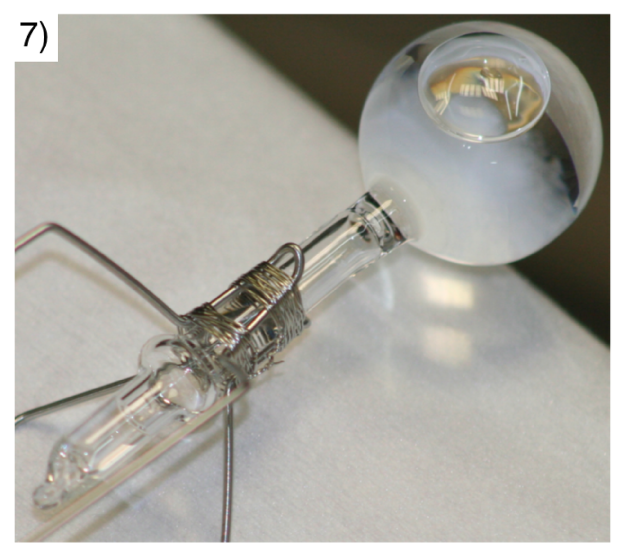


**$\beta^+$ calibration vial:** a micropipette within the standard vial will be used to minimise energy losses induced by glass vial (see Figure 5).
**neutron calibration holder:** 3 mm lead capsule contained inside of a delrin holder (lined with 5 mm of nickel) for $\gamma$ shielding purposes (see Figure 6).
**$\gamma$ and $^{222}$Rn calibration vial:** quartz sphere of 2.5 cm diameter with a neck for attachment; the calibration source is dissolved respectively in water and scintillator (see Figure 7).


[1] G. Alimonti et al., Nucl. Instr. Meth. **A** 600 (2011) [arXiv:0806.2400]
[2] G. Bellini et al., Phys. Rev. **D** (2014) 89:11 [arXiv:1308.0443]
[3] G. Bellini et al., JHEP (2013) **38** 1308 [arXiv:1304.7721]